

# Influence of reducing conditions of glass melting on phase transformations in zinc aluminosilicate glasses nucleated by titania

© O.S. Dymshits<sup>1</sup>, K.N. Ereemeev<sup>2</sup>, I.P. Alekseeva<sup>1</sup>, M.Ya. Tsenter<sup>1</sup>, L.R. Basyrova<sup>3</sup>, P.A. Loiko<sup>2</sup>, V.I. Popkov<sup>4</sup>, A.A. Zhilin<sup>5</sup>

<sup>1</sup> AO „Vavilov State Optical Institute“, St. Petersburg, Russia

<sup>2</sup> Centre de Recherche sur les Ions, les Matériaux et la Photonique (CIMAP), UMR 6252 CEA-CNRS-ENSICAEN, Université de Caen Normandie, Caen, France

<sup>3</sup> Université de Franche-Comté, CNRS, Institut FEMTO-ST, Besançon, France

<sup>4</sup> Ioffe Institute, St. Petersburg, Russia

<sup>5</sup> AO „D.V. Efremov Institute of Electrophysical Apparatus“ St. Petersburg, Russia

e-mail: vodym@goi.ru

Received November 29, 2024

Revised November 29, 2024

Accepted January 21, 2025

The influence of strongly reducing conditions of glass melting on phase transformations in titanium-containing glasses of the zinc aluminosilicate system has been investigated. The glass was melted with the addition of aluminium powder as a reducing agent. The glass-ceramics were obtained by heat treatments at temperatures ranging from 720°C to 1350°C. The processes of liquid phase separation and crystallization occurring in this glass during its secondary heat treatment were studied using structurally sensitive methods. The results are compared with the data for materials obtained under oxidizing conditions. It is shown for the first time that the sequence of phase transformations in glasses melted under strong reducing and oxidizing conditions is similar, but reducing conditions accelerate the gahnite crystallization and slow down the rutile and cristobalite crystallization, which indicates the entry of  $Ti^{3+}$  ions into the liquid phase separated zinc alumotitanate and zinc aluminate amorphous regions, as well as into the residual glass at the initial stages of phase decomposition. Broadband absorption of glass-ceramics in the visible and near-IR regions of the spectrum is caused by  $Ti^{3+}$  ions and  $Ti^{3+}-Ti^{4+}$  pairs in gahnite, rutile crystals and in the residual glass. Broadband luminescence of glass-ceramics was found to be due to  $Ti^{3+}$  ions and  $Ti^{3+}-Ti^{4+}$  pairs in gahnite nanocrystals rather than impurity  $Cr^{3+}$  ions, which was observed in glass melted under oxidizing conditions.

**Keywords:** glass-ceramics, red-ox conditions of glass melting, gahnite, rutile, absorption, luminescence.

DOI: 10.61011/EOS.2025.04.61413.7402-24

## Introduction








Glass-ceramics are composite materials obtained by controlled crystallization of glasses of special compositions, often with the addition of a nucleating agent (a glass component that promotes the formation of a functional crystalline phase in a residual glass) [1]. The first suggested nucleating agent is titania, and it remains the one most commonly used to this day [2]. Titanium is an ion of variable valence; therefore, a change in the redox conditions of glass melting, which is often needed to obtain optically active components in the required oxidation state, may affect the phase transformations initiated by the nucleator. Transparent glass-ceramics based on gahnite are a convenient object for investigating the influence of redox conditions of glass melting on the structure and properties of glass-ceramics, since one main phase crystallizes in them: zinc aluminate spinel (i.e., gahnite) [3–15]. The patterns of phase separation and crystallization in these glasses melted under oxidizing conditions have been studied in detail, and the phenomenon of three-phase immiscibility, which enables development of transparent glass-ceramics, was discovered

in them [9]. The influence of neutral [16] and weakly reducing [17] conditions of melting of these glasses on phase transformations in them and on the phase composition of the obtained glass-ceramics has also been examined. It was found that a change in the redox conditions of glass melting does not lead into a change in the structure of glass-ceramics, but causes a redistribution of  $Ti^{3+}$  and  $Ti^{4+}$  ions between the evolved phases, altering the optical properties of the obtained materials [16,17].

The aim of the present study is to examine the influence of strong reducing glass melting conditions on phase transformations in ceramizing glasses of the zinc aluminosilicate system. Such studies have not been conducted to date. This research is important for understanding the patterns involved in production of photonic materials that require different redox synthesis conditions.

## Objects and methods

Glass of the following composition was chosen for study: 23 ZnO, 23 Al<sub>2</sub>O<sub>3</sub>, 45.5 SiO<sub>2</sub>, 8.5 TiO<sub>2</sub> mol% [9]. It was melted under strong reducing (with added aluminum

Heat treatment mode, °C, 6 h	Glass	720,6	720+750	720+1000	720+1200	720+1300	720+1350
Image							

**Figure 1.** Photographs of transparent polished samples of the initial glass and glass-ceramics obtained by single and two-stage heat treatments 720°C, 6 h; 720°C, 6 h + 750°C, 6 h; 720°C, 6 h + 1000°C, 6 h (the sample thickness is 1 mm) and opaque samples obtained by the following heat treatments: 720°C, 6 h + 1200°C, 6 h; 720°C, 6 h + 1300°C, 6 h; and 720°C, 6 h + 1350°C, 6 h.

powder) and oxidizing (with added arsenic oxide) conditions. A detailed description of the synthesis procedure was provided in [17]. The prepared glasses were transparent, homogeneous, and free of bubbles and inclusions. Glass denoted as  $ZAS_{Al}$  (melted under reducing conditions) was violet colored (Fig. 1). Glass denoted as  $ZAS_{ox}$  (melted under oxidizing conditions) was light yellow in color [16]. These glasses were subjected to heat treatment in a Nabertherm annealing furnace with process parameters chosen based on the results of earlier studies [16].

Glass-ceramics obtained by heat treatment at temperatures up to and including 1050°C remained transparent. Transparent  $ZAS_{Al}$  glass-ceramics were colored black (Fig. 1), while transparent  $ZAS_{As}$  materials were light yellow [16]. Heat treatment at higher temperatures resulted in loss of transparency. Opaque  $ZAS_{Al}$  samples were blue in color and had a thin white crust. The  $ZAS_{Al}$  material produced by heat treatment at 1350°C was white in color, and its surface had a slight bluish tint (Fig. 1). All opaque  $ZAS_{As}$  samples were colored white [16]. Phase transformations in glass of the  $ZAS_{As}$  composition were discussed in detail in [16] and will be used here for reference.

Differential scanning calorimetry (DSC) curves were obtained using a Netzsch STA 449 F3 Jupiter calorimeter. See [17] for the details of the measurement procedure.

X-ray diffraction analysis of the samples was carried out using a Shimadzu 6000 diffractometer with Cu  $K\alpha$  ( $\lambda = 1.5406 \text{ \AA}$ ) radiation and a Ni filter. The measurement details were listed in [17]. To determine the lattice parameters of rutile (stable modification of  $TiO_2$ ) crystals, a special measurement was carried out within the range of angles  $2\theta = 26.9\text{--}27.6^\circ$  and  $2\theta = 53.8\text{--}54.6^\circ$  with a pitch of  $0.05^\circ$  and scan speed of  $2^\circ/\text{min}$  with a preset time of 100 s. The experimental details for measurement of lattice parameter  $a$  of gahnite were presented in [17]. The lattice parameters of rutile nanocrystals were determined from the diffraction peaks with Miller indices ( $hkl$ ) (110) and (211) at  $2\theta \sim 27.27^\circ$  and  $2\theta \sim 54.2^\circ$ , respectively [16]. The average size of gahnite and rutile crystals was determined by

examining the line with indices ( $hkl$ ) = (440)  $2\theta = 65.5^\circ$  (for gahnite) and the line with indices ( $hkl$ ) (110) at  $2\theta \sim 27.27^\circ$  (for rutile) using the Scherrer formula [18] with an accuracy of 5–10%.

An InVia Renishaw micro-Raman spectrometer was used to record Raman spectra (see [17] for procedure details). Photoluminescence spectra were measured with the same instrument and the same samples at  $\lambda_{exc} = 457 \text{ nm}$ . Absorption spectra were recorded with a Shimadzu UV 3600 spectrophotometer within the 190–3300 nm wavelength range with a pitch of 1 nm. The polished plates in these measurements were the same as those used to record the Raman and photoluminescence spectra. The methods for determining the absorption coefficient and the position of the absorption edge were outlined in [17].

## Results

The DSC curves of quenched glass  $ZAS_{Al}$  and the same glass heat-treated at 720°C for 6 h are shown in Fig. 2. The DSC curves of quenched and heat-treated glass  $ZAS_{As}$  are shown in the same figure to reveal the influence of redox conditions of glass melting on the crystallization kinetics.

Glass  $ZAS_{Al}$  heated in the DSC furnace to 1200°C is characterized by the presence of a single exothermic peak originated from the crystallization of zinc aluminate spinel [16,17]. A peak associated with the crystallization of the nucleating agent,  $TiO_2$ , was not detected in the DSC curve (apparently, due to the weak thermal effect of its crystallization from the liquid phase of phase-separated glass). The temperature parameters of glass transition and crystallization derived from the DSC data are presented in Table 1. According to the DSC data (Fig. 2), the crystallization of gahnite in the preliminary heat-treated sample proceeds at lower temperatures than in the initial glass; its glass transition temperature  $T_g$  also decreases. The shape of the exothermic crystallization peak changes (Table 1).

The DSC curves of  $ZAS_{Al}$  glass samples melted under strong reducing conditions differ from those of glass  $ZAS_{As}$

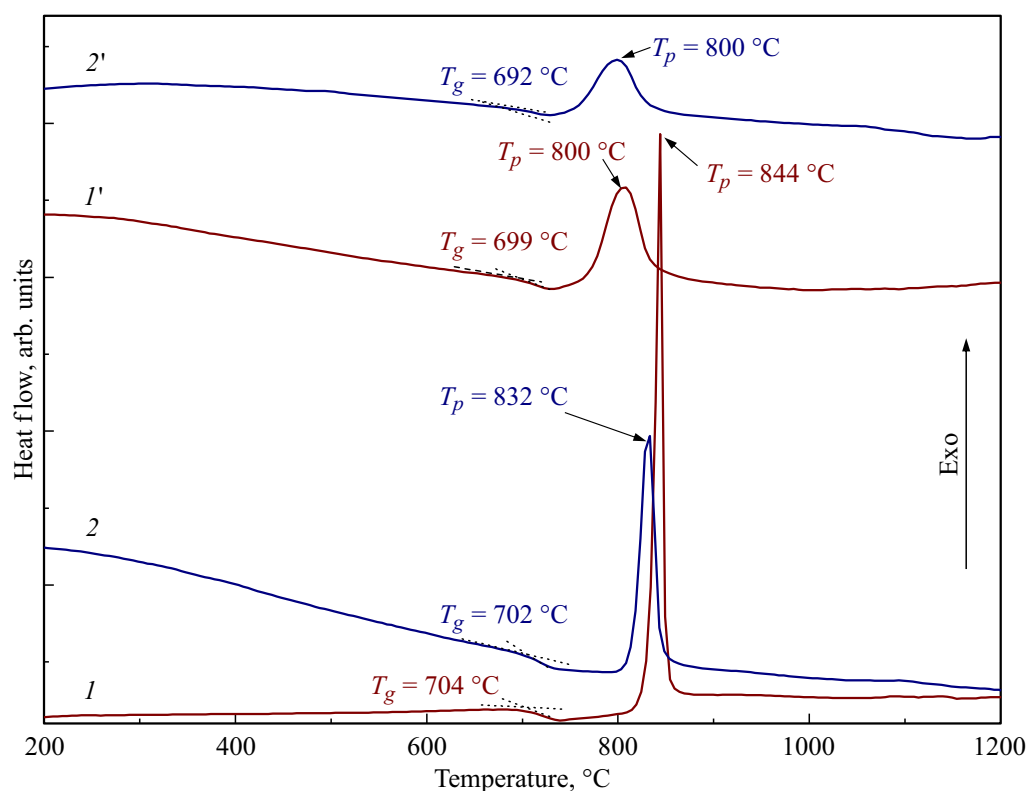


**Figure 2.** DSC curves of the glass  $ZAS_{ox}$  (1) and the  $ZAS_{ox}$  glass heat-treated at a temperature of 720°C for 6 h (1'); glass  $ZAS_{Al}$  (2) and the glass-ceramic obtained by the heat-treatment of glass  $ZAS_{Al}$  at 720°C for 6 h (2').

**Table 1.** Glass transition temperature ( $T_g$ ), crystallization onset temperature ( $T_x$ ), and temperature of the crystallization peak maximum ( $T_p$ ) of quenched and heat-treated  $ZAS_{Al}$  and  $ZAS_{As}$  glasses determined by analyzing the DSC curves

Heat treatment-schedule	$ZAS_{Al}$			$ZAS_{ox}$ [16]		
	$T_g$ , °C	$T_x$ , °C	$T_p$ , °C	$T_g$ , °C	$T_x$ , °C	$T_p$ , °C
—	702	820	832	704	822	844
720°C, 6 h	692	766	800	699	764	800

melted under oxidizing conditions (Fig. 2). The intensity of the exothermic peak of gahnite crystallization in the  $ZAS_{Al}$  glass is lower than in glass  $ZAS_{As}$ . This may be attributed to a reduction in the concentration of titania, which is the nucleator of gahnite crystallization, in this glass. The emergence of a weaker peak of gahnite crystallization in the  $ZAS_{Al}$  sample obtained by heat treatment at 720°C (compared to the peak in a similar  $ZAS_{As}$  sample) may be associated with partial precipitation of gahnite nanocrystals in the  $ZAS_{Al}$  sample in the course of this heat treatment (see below). The  $ZAS_{As}$  sample remained X-ray amorphous after heat treatment [16]. Thus, the influence of redox

conditions of the initial glass melting on the kinetics of its crystallization was revealed.

Figure 3 shows the XRD patterns of the initial  $ZAS_{Al}$  glass and glass-ceramics obtained by single- and two-stage heat treatments.

Crystals of the main crystalline phase (gahnite) 3.5 nm in size with lattice parameter  $a = 8.079 \text{ \AA}$ , which is somewhat lower than the reference value of this parameter  $a = 8.086 \text{ \AA}$  (ICDD PDF card #74-1136), form in glass as a result of heat treatment at a temperature of 720°C. Thus, heat treatment at this temperature leads to formation of a glass-ceramic, which explains the above-discussed features of the DSC curve. Gahnite crystallization in this sample is accompanied by a shift of the maximum of the amorphous halo from angle  $2\theta \cong 25.4^\circ$  in the XRD pattern of the initial glass to angle  $2\theta = 24.3^\circ$ . No peaks of gahnite nanocrystals and no shift of the maximum of the amorphous halo are seen in the diffraction pattern of the heat-treated sample melted under oxidizing and weak reducing conditions [16,17]. This suggests that the precipitation of the main crystalline phase is accelerated in glass melted under strong reducing conditions. Lattice parameter  $a$  of gahnite increases sharply to 8.100 Å after heat treatment at the second stage at 750°C and varies in a complex manner with a further increase in heat treatment temperature (see Table 2).

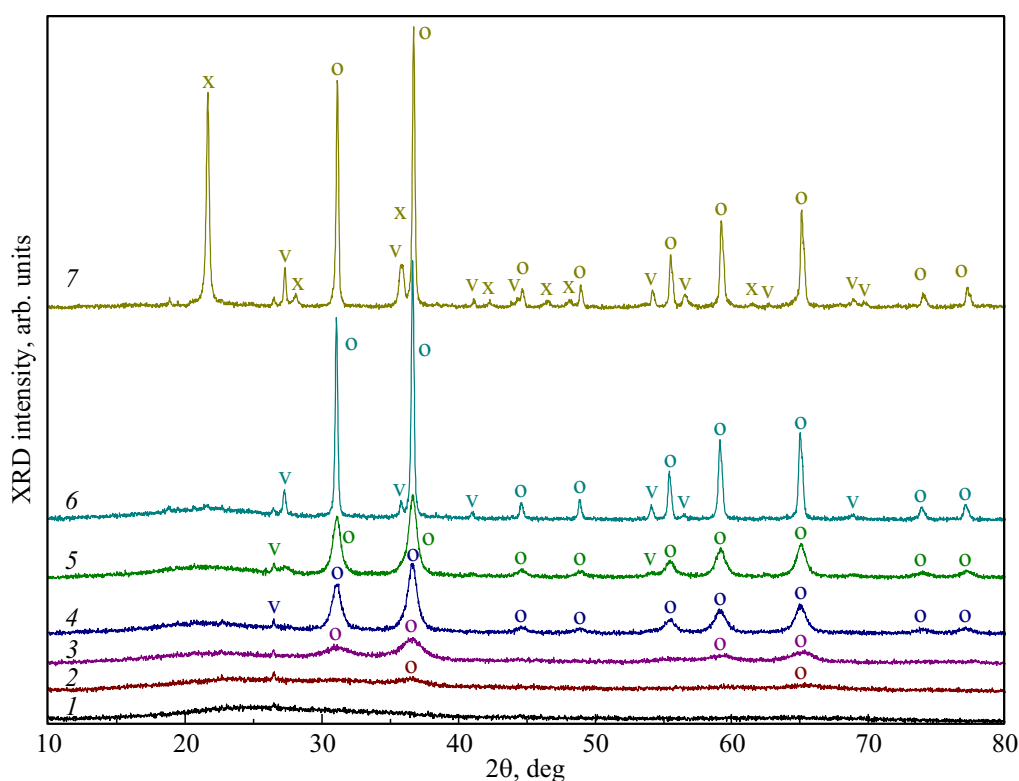


**Figure 3.** XRD patterns of the samples of initial glass (1) and glass-ceramics (2–7). Heat treatment schedules: 2 — 720°C, 6 h; 3 — 720°C, 6 h + 750°C, 6 h; 4 — 720°C, 6 h + 1000°C, 6 h; 5 — 720°C, 6 h + 1050°C, 6 h; 6 — 720°C, 6 h + 1300°C, 6 h; 7 — 720°C, 6 h + 1350°C, 6 h. Legend: o — gahnite crystals; v — rutile crystals; x — crystals of  $\alpha$ -cristobalite.

**Table 2.** Lattice parameters of gahnite and rutile nanocrystals and the average size of these crystals in glass-ceramics  $ZAS_{Al}$  and  $ZAS_{As}$

Heat treatment-schedule	$ZAS_{Al}$						$ZAS_{ox}$ [16]					
	$ZnAl_2O_4$		$TiO_2$				$ZnAl_2O_4$		$TiO_2$			
$^{\circ}C/6h$	$a \pm 0.0003, \text{\AA}$	$D, nm$	$a \pm 0.0003, \text{\AA}$	$c \pm 0.0003, \text{\AA}$	$D, nm$		$a \pm 0.0003, \text{\AA}$	$D, nm$	$a \pm 0.0003, \text{\AA}$	$c \pm 0.0003, \text{\AA}$	$D, nm$	
glass	—	—	—	—	—	—	—	—	—	—	—	—
720	8.079	3.5	—	—	—	—	—	—	—	—	—	—
720 + 750	8.100	6	—	—	—	8.085	5	—	—	—	—	—
720 + 800	8.102	7	—	—	—	8.105	6	—	—	—	—	—
720 + 850	8.116	7	—	—	—	8.111	7	—	—	—	—	—
720 + 900	8.118	8	—	—	—	8.109	8	—	—	—	—	—
720 + 950	8.115	9	—	—	—	8.108	9	—	—	—	—	—
720 + 1000	8.111	11	4.618	2.945	8	8.105	11	—	—	—	11	—
720 + 1050	8.108	14	4.618	2.949	19	8.105	16	4.613	2.959	14	—	—
720 + 1100	8.108	17	4.623	2.947	21	8.108	23	4.611	2.961	24	—	—
720 + 1200	8.108	31	4.616	2.947	30	8.110	40	4.611	2.957	38	—	—
720 + 1300	8.105	30	4.620	2.952	40	8.109	47	4.612	2.955	51	—	—
720 + 1350	8.090	31	4.613	2.947	46	8.105	49	4.613	2.958	51	—	—

It increases to a maximum value of 8.118 Å (heat treatment at 900°C), decreases to 8.108 Å as a result of heat treatment at 1050°C, remains virtually unchanged as the temperature grows to 1200°C, and drops to 8.090 Å after heat treatment at 1300°C (Fig. 4, *a*). The increase in lattice parameter of gahnite is attributable to the fact that  $Ti^{3+}$

ions occupy octahedral sites in the lattice, substituting  $Al^{3+}$  ions [16,17]. This is verified by the absorption spectra of these samples (see below). The lattice parameter of gahnite crystals in the  $ZAS_{As}$  samples (Table 2) changes in a similar fashion, suggesting that these crystals contain not only  $Ti^{3+}$  ions, but also  $Ti^{4+}$  ions. A similar lattice parameter

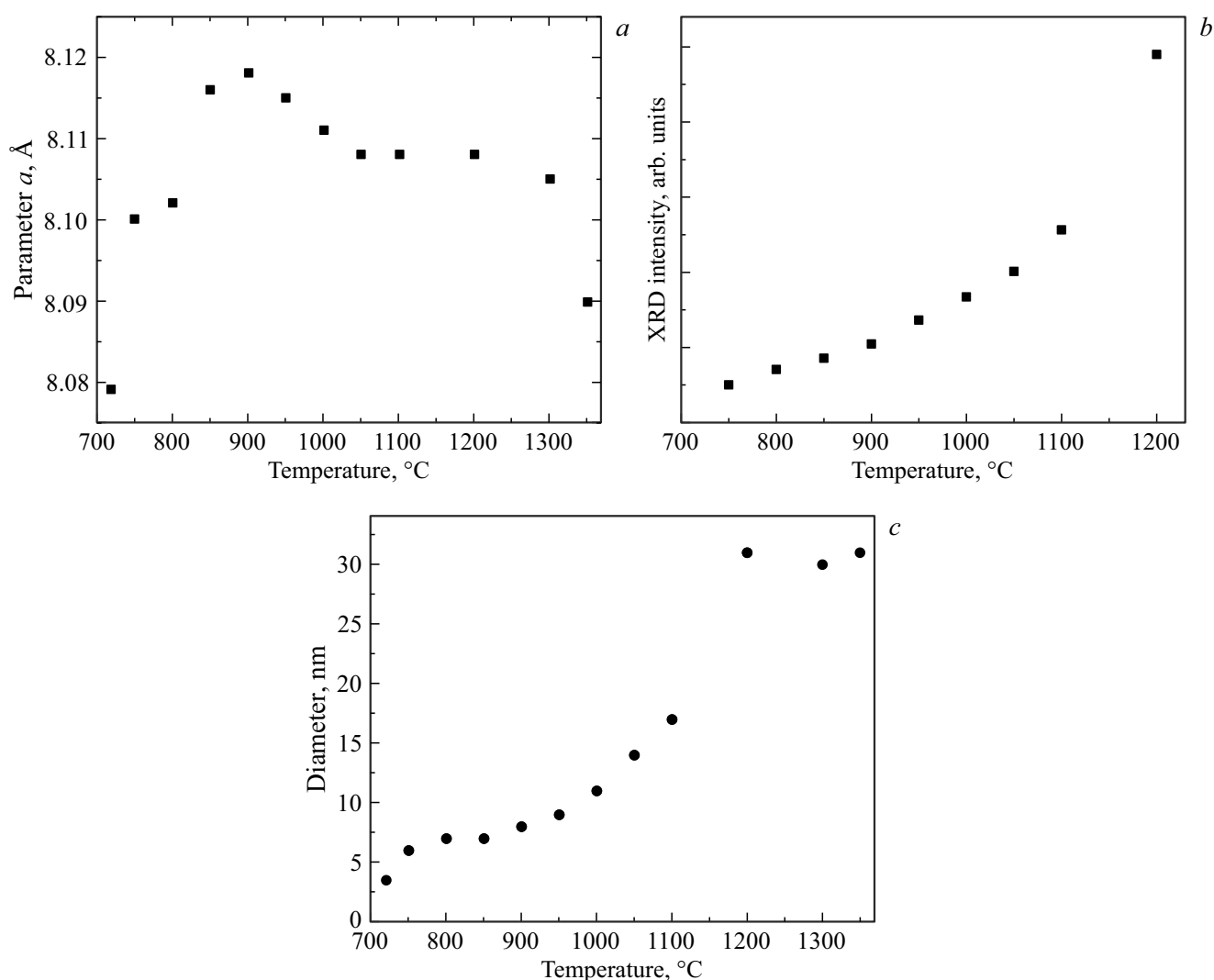


**Figure 4.** XRD data characterizing gahnite crystals in glass-ceramics ZAS<sub>Al</sub> with temperature increasing at the second stage of heat treatment: (a) lattice parameter  $a$  of gahnite; (b) intensity of the diffraction peak of gahnite with Miller index ( $hkl$ ) (311); and (c) average size of gahnite crystals. See text for heat treatment schedules.

reduction after heat treatment at temperatures above 900°C has been detected in earlier studies and was associated with the additional crystallization of gahnite during the decomposition of amorphous zinc aluminotitanate regions. One can assume that gahnite crystals precipitating from amorphous regions are noticeably depleted in titanium ions due to the crystallization of rutile [16]. The dependences of the volume fraction of gahnite crystals and their average size on the heat treatment temperature are presented in Fig. 4, *b* and Fig. 4, *c*, respectively, and in Table 2.

Traces of rutile (a stable modification of titania) were found in the sample heat-treated at a temperature of 1000°C (Fig. 3). The amount of rutile and the average crystal size increase as the heat treatment temperature increases from 1000°C to 1300°C; the average crystal size grows from ~8 nm to ~46 nm in the process. The lattice parameters and average crystal sizes of gahnite and rutile are listed in Table 2.

Rutile has a chain structure. Straight chains are formed by TiO<sub>6</sub> octahedra. Octahedra are edge-linked in the rutile structure, and a chain is formed by the interlocking of edge-linked octahedra at their vertices. These chains are extended along axis  $c$ . Parameter  $c$  of the rutile cell is thus related to the length of an octahedron edge in a chain, and parameter  $a$  is the double thickness of an octahedron. The values of rutile parameters may change as a result of distortion of octahedra and changes in their sizes and as a result of changes in the coupling of octahedra in a chain due to isomorphic substitutions. For example, when Ti<sup>4+</sup> is substituted with Ti<sup>3+</sup> in rutile octahedra, parameters  $a$  and  $c$  are doubled, chains transform into zigzag ones, and even a reduction in symmetry (i.e., the formation of brookite) is observed. The values of parameters  $a$  and  $c$  of the rutile cell obtained in the present study do not depend on the heat treatment temperature. However, their values deviate from the reference ones and differ in glasses obtained

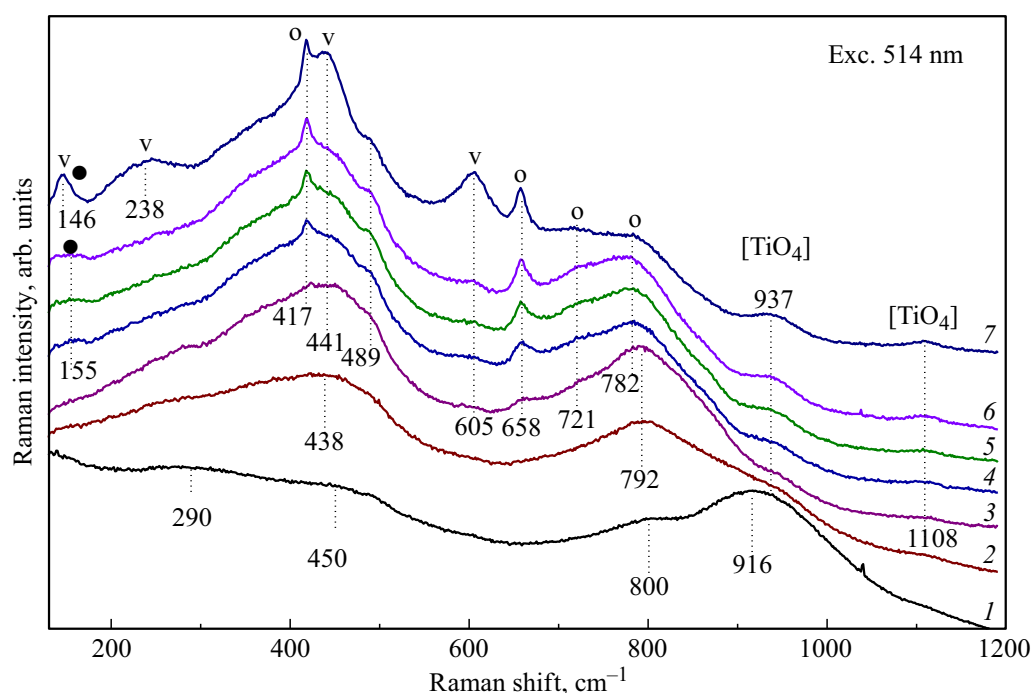


**Figure 5.** Raman spectra of the samples of initial glass (1) and glass-ceramics (2–7). Heat treatment schedules: 2 — 720°C, 6 h; 3 — 720°C, 6 h + 750°C, 6 h; 4 — 720°C, 6 h + 850°C, 6 h; 5 — 720°C, 6 h + 900°C, 6 h; 6 — 720°C, 6 h + 950°C, 6 h; 7 — 720°C, 6 h + 1000°C, 6 h. The excitation wavelength is indicated in the figure. Legend: o — vibrations in gahnite crystals; • — vibrations in anatase crystals; v — vibrations in rutile crystals.

under different redox conditions. According to ICDD card #82-0147 for rutile, parameter  $a = 4.593 \text{ \AA}$ ,  $c = 2.957 \text{ \AA}$ . Notably, parameters  $c$  of rutile in the  $\text{ZAS}_{\text{As}}$  samples are close to the reference ones, while the values of parameters  $a$  are  $\sim 0.02 \text{ \AA}$  higher. In the  $\text{ZAS}_{\text{Al}}$  samples, parameters  $a$  are  $\sim 0.01 \text{ \AA}$  lower, and parameters  $c$  are  $\sim 0.025 \text{ \AA}$  higher than the reference ones. The difference in parameter values exceeds the error of their determination. Therefore, it is worth saying that redox conditions of glass smelting affect the structure of rutile.

The position of the amorphous halo continues to shift with increasing heat treatment temperature, reaching a diffraction angle  $2\theta \cong 22.0^\circ$  in the XRD pattern of the sample obtained by heat treatment at 900°C at the second stage. A further increase in heat treatment temperature has no effect on the halo; it shifts to angle  $2\theta \cong 21.8^\circ$  only after heat treatment at 1300°C. This position of the amorphous halo indicates that the composition of high-silicate residual glass is close to that of quartz glass [9]. The amorphous halo vanishes during crystallization of  $\alpha$ -cristobalite at a temperature of 1350°C, when the phase composition of the  $\text{ZAS}_{\text{Al}}$  material is represented by stable phases of gahnite, rutile, and  $\alpha$ -cristobalite.

Since the processes of liquid phase separation in titanium-containing glasses cannot be probed by X-ray diffraction analysis, Raman spectroscopy is an indispensable method for their monitoring. This is especially true for ceramizing glasses of the zinc aluminosilicate system [9,12,16,19–

22], wherein the zinc aluminotitanate amorphous phase crystallizes only at heat treatment temperatures upward of 1000°C. The lack of titanate crystalline phases and the impossibility of monitoring of liquid phase separation in the titanium-containing amorphous phase due to the lack of Raman data forced researchers to assume that titanium ions in such glass-ceramics are contained in noticeable amounts in gahnite crystals, which form solid solutions  $\text{ZnAl}_2\text{O}_4\text{--Zn}_2\text{TiO}_4$  [7].

In the present study, the development of liquid phase separation was examined using Raman spectroscopy (Fig. 5). The Raman spectrum of the initial glass contains broad poorly resolved bands at  $\sim 290 \text{ cm}^{-1}$ ,  $\sim 450 \text{ cm}^{-1}$ , and  $\sim 800 \text{ cm}^{-1}$ , which correspond to vibrations of the aluminosilicate matrix, and an intense band with a maximum at  $\sim 916 \text{ cm}^{-1}$  induced by  $[\text{TiO}_4]$  tetrahedra in this aluminosilicate matrix [9,19]. A significant change in the Raman spectrum of the initial glass as a result of heat treatment at a temperature of 720°C is indicative of liquid phase separation [9,19]. The spectrum features two broad bands with maxima at  $\sim 438 \text{ cm}^{-1}$  and  $792 \text{ cm}^{-1}$ , and a high-frequency band in the region of  $940 \text{ cm}^{-1}$  is also discernible. The data from [9,19] suggest that the intense band with a maximum at  $\sim 792 \text{ cm}^{-1}$  may be associated with vibrations of groups of octahedrally and pentacoordinated  $\text{Ti}^{4+}$  ions in the liquid phase separated zinc aluminotitanate regions [9,19]. Note that the emergence of gahnite crystals under heat treatment, which was detected



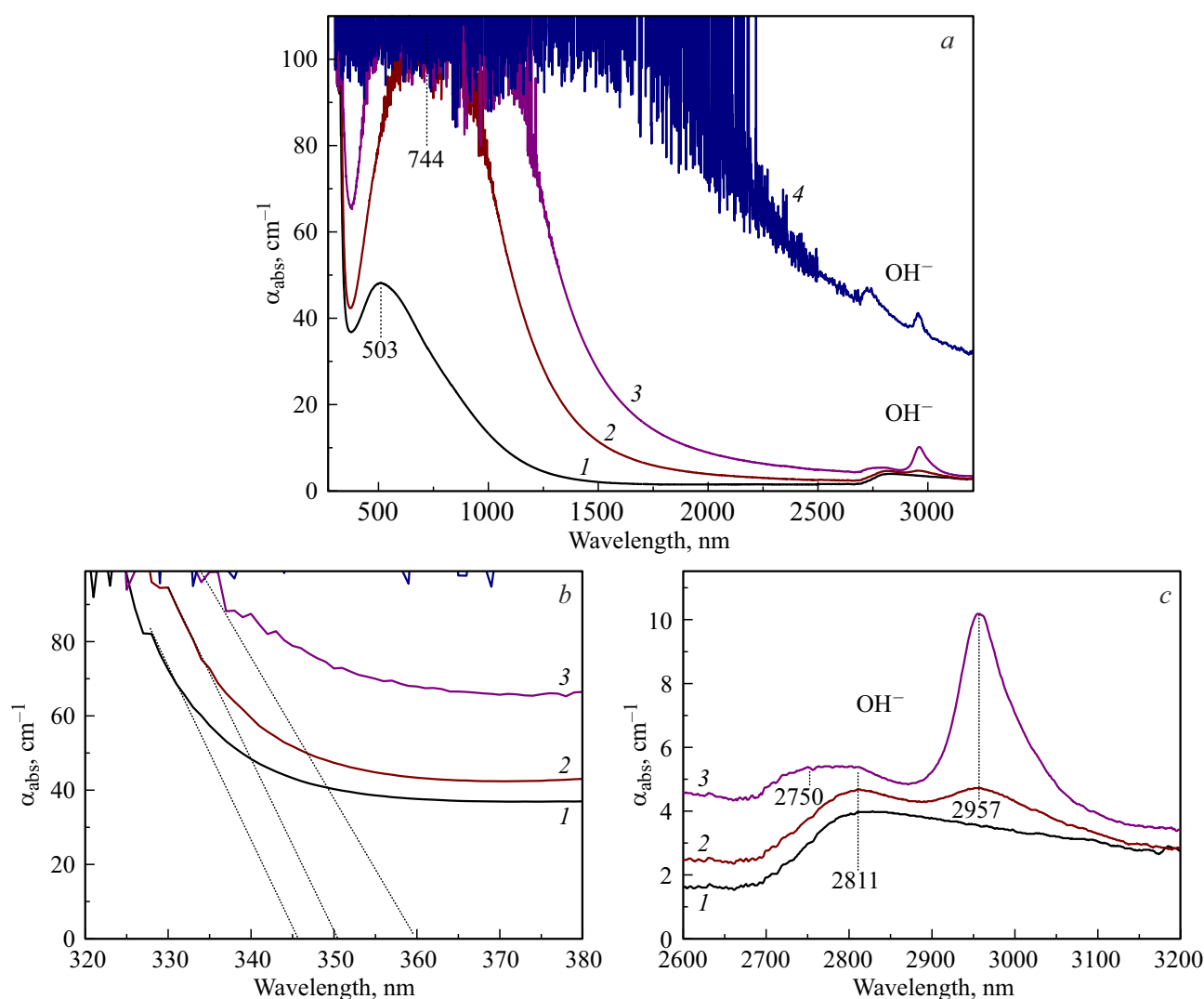


**Figure 6.** Absorption spectra of the initial (1) and heat-treated (2–4) glass ZAS<sub>Al</sub> samples: (a) within the spectral range from 270 nm to 3200 nm; (b) within the spectral range from 320 nm to 380 nm; and (c) within the spectral range from 2600 nm to 3200 nm. Heat treatment schedules: 2 — 720°C, 6 h; 3 — 720°C 6 h + 750°C, 6 h; 4 — 720°C, 6 h + 1000°C, 6 h.

by XRD analysis, is not revealed by Raman spectroscopy, since this method is less sensitive to the formation of crystals with a spinel structure. Note also that the liquid phase separation detected by Raman spectroscopy and the onset of gahnite crystallization, which was detected by XRD data, provide an explanation for the significant changes in characteristic temperatures and the shape of the gahnite crystallization peak in the DSC curve of this sample (Fig. 2).

The Raman spectra of samples heat-treated at the second stage at temperatures within the 750–1000°C range are indicative of further development of processes that were initiated during single-stage heat treatment. This implies that structuring proceeds in already formed liquid phase separated regions and residual glass. Gahnite bands emerge and grow, which is evidenced by the bands with maxima at 417  $\text{cm}^{-1}$ , 658  $\text{cm}^{-1}$ , 721  $\text{cm}^{-1}$ , and 782  $\text{cm}^{-1}$ . It has been demonstrated earlier that the formation of bands with

maxima at  $\sim 720 \text{ cm}^{-1}$  and  $\sim 780 \text{ cm}^{-1}$  may be attributed to the entry of titanium ions, which occupy octahedral sites, into gahnite crystals [22]. A broad weak band with a maximum at  $\sim 155 \text{ cm}^{-1}$  corresponding to the most intense vibration in anatase crystals [23], which cannot be revealed by XRD study due to the small amount of this phase, emerges in the spectrum of the sample heat-treated at 850°C. Note that this band was not observed in the Raman spectra of the sample obtained under weak reducing conditions [17]. The intensity of the anatase band does not change with heat treatment temperature, but this band is not detected in the spectrum of the sample obtained by heat treatment at 1000°C. This spectrum features vibrations of rutile crystals [9] at 146  $\text{cm}^{-1}$ ,  $\sim 238 \text{ cm}^{-1}$ , 441  $\text{cm}^{-1}$ , and 605  $\text{cm}^{-1}$ , which agrees with the XRD data. The broad band with a maximum at 792  $\text{cm}^{-1}$  gets weaker gradually. It is almost indiscernible in the spectrum

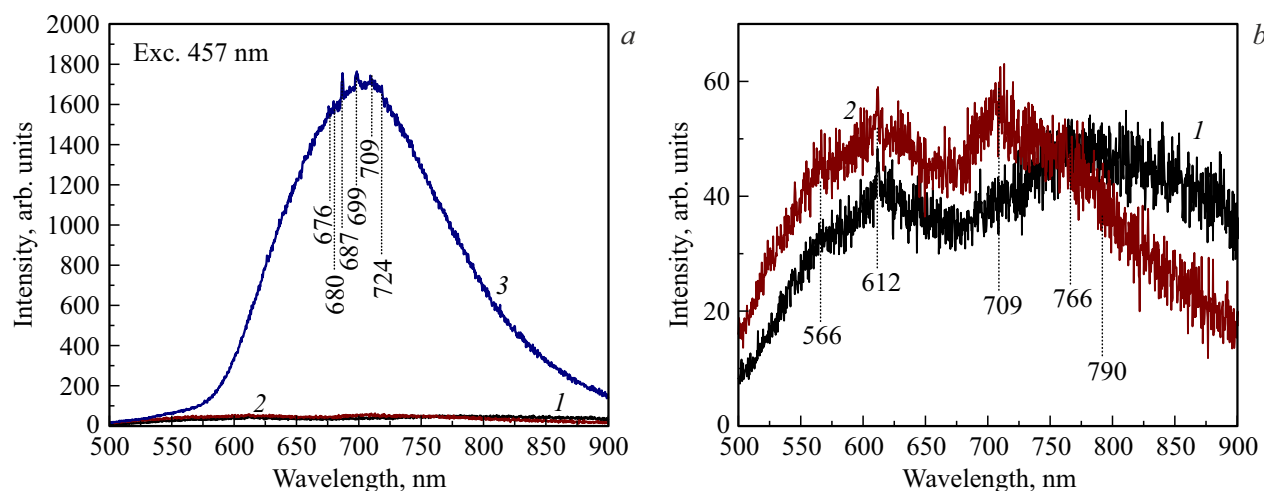


**Figure 7.** (a) Luminescence spectra of the initial ZAS<sub>Al</sub> glass (1) and glass-ceramics. Heat treatment schedules: 720°C, 6 h (2), 720°C, 6 h + 1000°C, 6 h (3). (b) Luminescence spectra (plotted on a reduced scale) of the initial ZAS<sub>Al</sub> glass (1) and the glass-ceramic produced by heat treatment at 720°C, 6 h (2). The excitation wavelength is indicated in Fig. 7, a.

of the sample obtained by heat treatment at 1000°C in which the precipitation of rutile nanocrystals was detected. The gradually intensifying broad bands with maxima at  $\sim 937\text{ cm}^{-1}$  and  $\sim 1108\text{ cm}^{-1}$  correspond to  $[\text{TiO}_4]$  groups in high-silicate residual glass [19]. Thus, in accordance with the XRD data and in addition to these data, the spectrum of the sample obtained by heat treatment at 1000°C, was found to contain vibrations induced by crystals of titanium-containing gahnite, rutile, and  $[\text{TiO}_4]$  groups in residual glass. The sequence and nature of phase transformations in the titanium-containing amorphous phase during the crystallization of gahnite and in the residual glass phase are close to those reported for glasses melted under oxidizing, neutral, and weak reducing conditions [9,16,17]. We failed to find any features associated with  $\text{Ti}^{3+}$  ions in the Raman spectra. The authors of [24] made a similar conclusion: they found only an intense band in the region of  $935\text{ cm}^{-1}$  caused by vibrations of Si–O–Ti bonds in the Raman spectra of quartz glasses doped with  $\text{Ti}^{4+}$  and  $\text{Ti}^{3+}$  ions.

According to Figs. 6, a, b, the absorption edge in the spectrum of glass of the ZAS<sub>Al</sub> composition is at a wavelength of 346 nm. The position of the absorption edge in titanium-containing glasses is often associated with charge transfer bands between titanium ions in various oxidation states and oxygen ions. The charge transfer band between  $\text{Ti}^{3+}$  and  $\text{O}^{2-}$  ions is located in the ultraviolet spectral region within the  $\sim 240\text{--}260\text{ nm}$  wavelength range [25,26]. The charge transfer band between  $\text{Ti}^{4+}$  and  $\text{O}^{2-}$  ions is usually localized in the region of 300 nm, and its long-wavelength edge extends to 400 nm [27]. Thus, the absorption edge of glass ZAS<sub>Al</sub> is largely determined by the O–Ti<sup>4+</sup> charge-transfer band. An intense asymmetric absorption band with a maximum at  $\sim 503\text{ nm}$ , which extends into the near IR region of the spectrum and is induced by absorption of  $\text{Ti}^{3+}$  ions in distorted octahedral ( ${}^2T_{2g} \rightarrow E_g$  transition) coordination [16,17,26–28] and in  $\text{Ti}^{3+}\text{--Ti}^{4+}$  ion pairs, is

found in the spectrum of glass ZAS<sub>Al</sub> [17,29–31]. A broad unstructured absorption band of OH groups is located in the 2650–3300 nm region.

The absorption edge in the spectrum of the glass-ceramic obtained by single-stage heat treatment at 720°C is positioned at a wavelength of 351 nm. The spectrum is dominated by a broad and intense absorption band with a maximum at 744 nm and its long-wavelength absorption edge extending to  $\sim 2000\text{ nm}$ . Since the XRD data revealed gahnite nanocrystals precipitation in this sample and, according to the Raman spectroscopy data, titanium-containing liquid phase separated regions did also form in it, the observed spectral changes may be associated with the entry of  $\text{Ti}^{3+}$  ions in octahedral coordination ( ${}^2T_{2g} \rightarrow E_g$  transition) and in the form of  $\text{Ti}^{3+}/\text{Ti}^{4+}$  pairs into these phases [16,17]. The absorption band of OH groups undergoes structuring, which is a spectral sign of gahnite crystallization [16].

Following heat treatment at the second stage at a temperature of 750°C, the absorption edge shifts further toward longer wavelengths (to 360 nm; see Fig. 6, b). The absorption band in the visible and near IR spectral region broadens (Fig. 6, a), while the position of its maximum apparently remains unchanged. The structuring of the absorption band of OH groups continues (Fig. 6, c). These spectral changes correlate with the ongoing formation of titanium-containing gahnite nanocrystals (Figs. 3 and 5), and the amorphous zinc aluminotitanate phase (Fig. 5). The absorption of the sample obtained by two-stage heat treatment with a temperature of 1000°C at the second stage extends over the entire recorded spectral region (up to 2200 nm). Since the XRD and Raman data reveal additional crystallization of rutile in these samples, this band may be formed not only by the absorption of octahedrally coordinated  $\text{Ti}^{3+}$  ions and  $\text{Ti}^{3+}/\text{Ti}^{4+}$  pairs [28] in gahnite nanocrystals, but also by the absorption of  $\text{Ti}^{3+}$  ions in rutile



nanocrystals. Indeed, according to [32] and the references therein, the spectrum of dark blue rutile, the color of which is due to impurity  $\text{Ti}^{3+}$  ions and  $\text{Ti}^{3+}/\text{Ti}^{4+}$  pairs, has an absorption edge at  $\sim 412\text{ nm}$ , weak bands in the visible region, and intense absorption in the IR region of the spectrum within the wavelength interval from  $\sim 800\text{ nm}$  to  $\sim 3300\text{ nm}$  with a maximum at  $1400\text{--}1660\text{ nm}$  (with the absorption of OH groups superimposed on it).

According to Fig. 6, *a*, a structured absorption band of OH groups is seen on the wing of the absorption band of the  $\text{ZAS}_{\text{Al}}$  glass-ceramic sample that decreases smoothly in the  $2200\text{--}3200\text{ nm}$  spectral region. The measured luminescence spectra of the initial glass, glass heat-treated at a temperature of  $720^\circ\text{C}$  (single-stage heat treatment), and glass processed at  $1000^\circ\text{C}$  at the second stage (Fig. 7) differ fundamentally from the ones recorded earlier for samples of this composition obtained from glasses melted under oxidizing, neutral, and weak reducing conditions [16,17]. The very weak broad luminescence band of the initial glass has maxima at  $\sim 566\text{ nm}$ ,  $\sim 612\text{ nm}$ ,  $\sim 709\text{ nm}$ , and  $\sim 790\text{ nm}$ . The luminescence intensity of the glass-ceramic obtained by heat treatment at  $720^\circ\text{C}$  does not change relative to the luminescence intensity of the initial glass, although the band gets slightly narrower due to a reduction in its intensity in the  $760\text{--}900\text{ nm}$  region. A broad intense luminescence band in the region from  $555\text{ nm}$  to  $900\text{ nm}$  with narrow peaks on its profile at wavelengths of  $676$ ,  $680$ ,  $687$ ,  $699$ ,  $709$ , and  $724\text{ nm}$  was recorded in the  $\text{ZAS}_{\text{Al}}$  glass-ceramic obtained by crystallization at a temperature of  $1000^\circ\text{C}$  at the second stage.

## Discussion

The phase transformations in glass of the studied composition ( $\text{ZAS}_{\text{As}}$ ) melted under oxidizing conditions have already been examined using a set of structure-sensitive methods in [9,19]. It was found that the high content of titanium ions in the highest oxidation state in all melted glasses makes the nature of crystalline phases in them independent of the melting conditions, since the concentration of the nucleating agent sets the sequence and nature of the phase transitions in the process of ceramization of these glasses. The results obtained in the present study verify the validity of these patterns. A comparison of the Raman spectra of the initial  $\text{ZAS}_{\text{As}}$  and  $\text{ZAS}_{\text{Al}}$  glasses (not shown here) reveals that the intensity of the band in the region of  $900\text{ cm}^{-1}$  is higher in the spectrum of  $\text{ZAS}_{\text{As}}$ , and its position is shifted slightly toward the region of higher wave numbers relative to this band in the spectrum of glass  $\text{ZAS}_{\text{Al}}$ . This is indicative of acceleration of the processes of liquid phase separation in glass melted under reducing conditions. Nevertheless, it may be assumed that titanium ions in the highest oxidation state are also dominant in the  $\text{ZAS}_{\text{Al}}$  glass, establishing the traditional sequence of phase transformations during heat treatment of the initial glass.

A comparison of the results of DSC, XRD, Raman, and absorption and luminescence spectroscopy studies of phase transformations, structure, and optical properties of glasses melted under reducing and oxidizing conditions and glass-ceramics based on them revealed that the sequences of phase transformations in glasses melted under reducing and oxidizing conditions are similar; however, reducing synthesis conditions accelerate the crystallization of gahnite (Fig. 8, *a*) and slow down the crystallization of rutile (Fig. 8, *b*) and  $\alpha$ -cristobalite (Fig. 8, *c*), which indicates that  $\text{Ti}^{3+}$  ions enter the liquid phase separated zinc aluminotitanate and zinc aluminate amorphous regions and residual high-silicate glass at the initial stages of phase separation. It is demonstrated in Fig. 8 that the precipitation of gahnite nanocrystals is accompanied by structuring of the absorption band of OH groups, which is indicative of their localization on the surface of these crystals [16].

It has been reported earlier that chromium ions present in glass in the form of uncontrolled batch impurities demonstrate noticeable luminescence both in the initial glasses melted under oxidizing, neutral, and weak reducing conditions and in the corresponding glass-ceramics and are incorporated into the structure of gahnite crystals [16,17]. The  $\text{ZAS}_{\text{Al}}$  materials obtained in the present study differ significantly from those prepared earlier in that they contain more titanium ions in the oxidation state of  $3+$ , which is attributable to the strong reducing conditions of their melting. This difference is evident not only in the absorption spectra of glass and glass-ceramics, but also in their luminescence spectra, which differ fundamentally from those presented in [16,17]. The luminescence spectrum of the initial glass is close in shape to the luminescence spectrum of titanium-containing calcium aluminosilicate glass obtained in [33] that features a band with a maximum at  $673\text{ nm}$ , which is induced by the  ${}^2E \rightarrow {}^2T_2$  transition in octahedrally coordinated  $\text{Ti}^{3+}$  ions [33], and a band with a maximum at  $790\text{ nm}$ , which is associated with the interaction of  $\text{Ti}^{3+}$  ions with structural defects,  $\text{Ti}^{4+}$  ions, or impurity (e.g., iron) ions [33]. It is the first time that the luminescence of  $\text{Cr}^{3+}$  ions in the initial  $\text{ZAS}_{\text{Al}}$  glass and the glass-ceramic obtained by heat treatment at  $720^\circ\text{C}$  has not been detected. The narrowing of the luminescence peak of titanium ions after heat treatment at a temperature of  $720^\circ\text{C}$  and the emergence of intense broadband luminescence in a glass-ceramic containing a large volume fraction of gahnite nanocrystals are indicative of the luminescence of  $\text{Ti}^{3+}$  ions [27–31,33–37] in these crystals. Such results have never been reported before. Weak narrow peaks seen against the background of a broad band correspond to weak luminescence of chromium ions at octahedral  $O_h$  sites in gahnite nanocrystals [16,17], which was dominant in  $\text{ZAS}_{\text{As}}$  glass-ceramics melted under oxidizing conditions and got suppressed in  $\text{ZAS}_{\text{Al}}$  glass-ceramics obtained under strong reducing conditions. The mechanisms of this phenomenon will be the subject of further study.

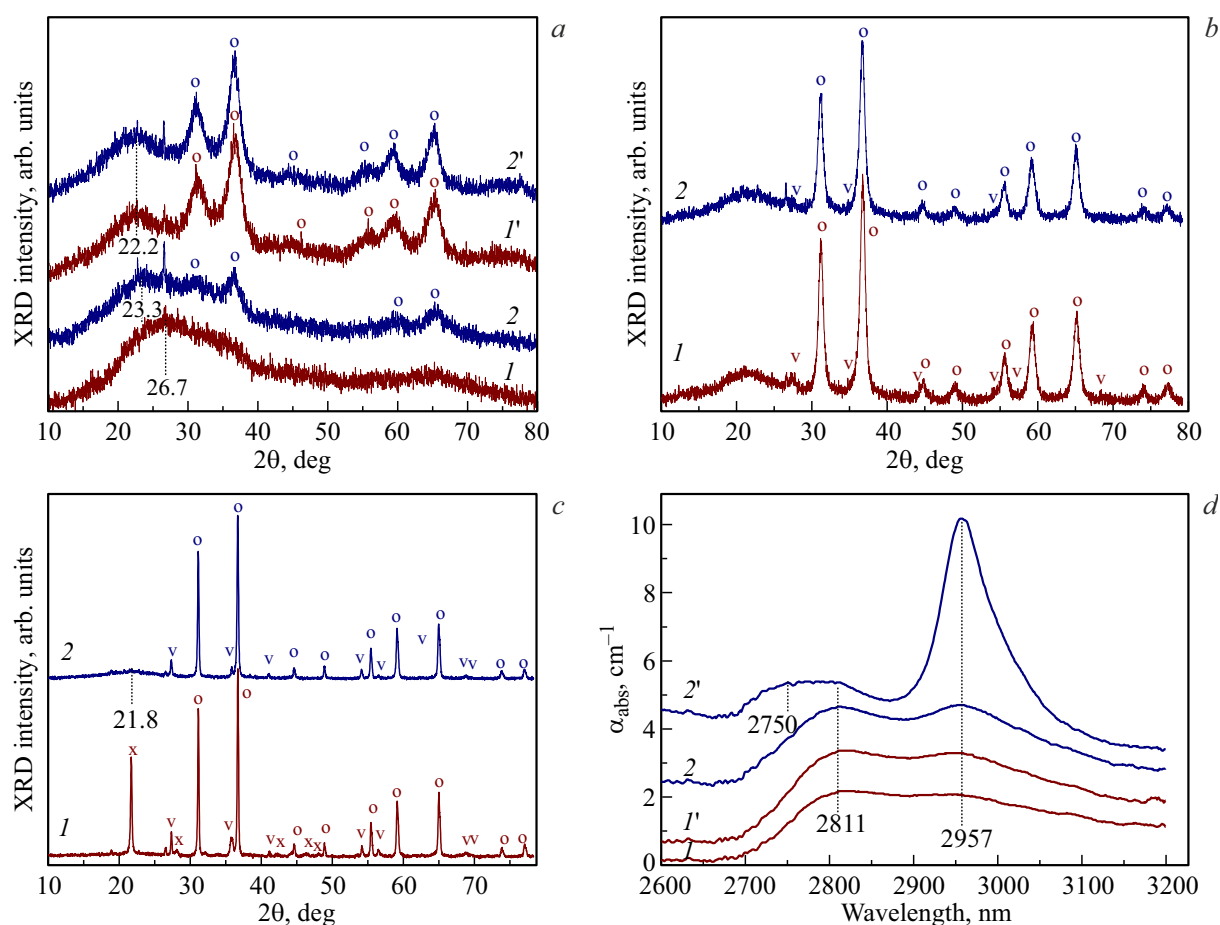


**Figure 8.** XRD patterns (*a–c*) and absorption spectra (*d*) of glass-ceramics: *1* and *1'* — ZAS<sub>Al</sub>; *2* and *2'* — ZAS<sub>As</sub>. Heat treatment schedules (*a, d*): *1, 2* — 720°C, 6 h; *1', 2'* — 720°C, 6 h + 750°C, 6 h; (*b*) 720°C, 6 h + 1000°C, 6 h; (*c*) 720°C, 6 h + 1300°C, 6 h. Legend: o — gahnite crystals; v — rutile crystals; x —  $\alpha$ -cristobalite crystals.

## Conclusions

The influence of strong reducing melting conditions on phase transformations in titanium-containing ceramizing glasses of the zinc aluminosilicate system was studied. It was found that the strong reducing conditions of the initial glass melting do not lead to a change in the phase composition of the resulting glass-ceramics, which is potentially beneficial for the production of glass-ceramics containing ions of variable valence in lower oxidation states.

It was found out that the strong reducing conditions of the initial glass melting affect the kinetics of phase transformations, lowering the temperature of gahnite crystallization and raising the temperature of rutile and  $\alpha$ -cristobalite crystallization. This is attributable to the entry of  $\text{Ti}^{3+}$  ions into the liquid phase separated zinc aluminotitanate and zinc aluminate amorphous regions and into residual high-silicate glass at the initial stages of phase separation.

The increase in lattice parameter of gahnite crystals precipitating during heat treatment of glass within the temperature range of 720–1350°C indicates entering of titanium ions  $\text{Ti}^{3+}$  and  $\text{Ti}^{4+}$  in their composition.

The absorption spectrum of the initial glass is indicative of the presence of  $\text{Ti}^{3+}$  ions in the octahedral ligand field and  $\text{Ti}^{3+}/\text{Ti}^{4+}$  pairs. The absorption spectra of glass-ceramics revealed an increase in absorption intensity, which is caused by these color centers in the crystalline and amorphous phases of these multiphase materials.

Intense broadband luminescence in the 550–900 nm spectral region, which is induced by  $\text{Ti}^{3+}$  ions in the crystalline phase of gahnite, has been observed for the first time in glass-ceramics based on gahnite nanocrystals with a spinel structure.

## Conflict of interest

The authors declare that they have no conflict of interest.

## References

- [1] J. Deubener, M. Allix, M.J. Davis, A. Duran, T. Höche, T. Honma, T. Komatsu, S. Krüger, I. Mitra, R. Müller, S. Nakane, M.J. Pascual, J.W.P. Schmelzer, E.D. Zanotto, S. Zhou. *J. Non-Cryst. Solids*, **501**, 3–10 (2018). DOI:10.1016/j.jnoncrysol.2018.01.033

- [2] S.D. Stookey. Method of Making Ceramics and Product Thereof, U.S. Pat. No. 2,920,971, January 12, 1960.
- [3] G.H. Beall, D.A. Duke. *J. Mater. Sci.*, **4**, 340–352 (1969). DOI: 10.1007/BF00550404
- [4] A.J. Stryjak, P.W. McMillan. *J. Mater. Sci.*, **13**, 1794–1804 (1978). DOI: 10.1007/BF00548743
- [5] Z. Strnad. *Glass-Ceramic Materials* (Elsevier, Amsterdam, The Netherlands, 1986), p. 101–105.
- [6] L.R. Pinckney. Transparent glass-ceramics containing gahnite. U.S. Patent No. 4,687,750; 1987.
- [7] L.R. Pinckney. *J. Non-Cryst. Solids*, **255**, 171–177 (1999). DOI: 10.1016/S0022-3093(99)00368-3
- [8] G.H. Beall, L.R. Pinckney. *J. Am. Ceram. Soc.*, **82**, 5–16 (1999). DOI: 10.1111/j.1151-2916.1999.tb01716.x
- [9] V.V. Golubkov, O.S. Dymshits, V.I. Petrov, A.V. Shashkin, M.Ya. Tsenter, A.A. Zhilin, U. Kang. *J. Non-Cryst. Solids*, **351**, 711 (2005). DOI: 10.1016/j.jnoncrysol.2005.01.071
- [10] E. Tkalčec, S. Kurajica, H. Ivanković. *J. Non-Cryst. Solids*, **351**, 149–157 (2005). DOI: 10.1016/j.jnoncrysol.2004.09.024
- [11] A.R. Molla, A.M. Rodrigues, S.P. Singh, R.F. Lancelotti, E.D. Zanotto, A.C.M. Rodrigues, M.R. Dousti, A.S.S. de Camargo, C.J. Magon, I.A.A. Silva. *J. Am. Ceram. Soc.*, **100**, 1963–1975 (2017). DOI: 10.1111/jace.14753
- [12] P. Loiko, A. Belyaev, O. Dymshits, I. Evdokimov, V. Vitkin, K. Volkova, M. Tsenter, A. Volokitina, M. Baranov, E. Vilejshikova, A. Baranov, A. Zhilin. *J. Alloys Compd.*, **725**, 998–1005 (2017). DOI: 10.1016/j.jallcom.2017.07.239
- [13] A.L. Mitchel, D.E. Perea, M.G. Wirth, J.V. Ryan, R.E. Youngman, A. Rezikyan, A.J. Fahey, D.K. Schreiber. *Scr. Mater.*, **203**, 114110 (1–6) (2021). DOI: 10.1016/j.scriptamat.2021.114110
- [14] S. Kurajica, J. Šipušić, M. Zupancic, I. Brautović, M. Albrecht. *J. Non-Cryst. Solids*, **553**, 120481(1–8) (2021). DOI: 10.1016/j.jnoncrysol.2020.120481
- [15] Y. Guo, Y. Lu, C. Liu, J. Wang, J. Han, J. Ruan. *Alloys Compd.*, **851**, 156891(1–8) (2021). DOI: 10.1016/j.jallcom.2020.156891
- [16] K. Ereemeev, O. Dymshits, I. Alekseeva, A. Khubetsov, S. Zapalova, M. Tsenter, L. Basyrova, J.M. Serres, X. Mateos, P. Loiko, V. Popkov, A. Zhilin. *J. Eur. Ceram. Soc.*, **44**, 3362 (2024). DOI: 10.1016/j.jeurceramsoc.2023.12.026
- [17] K.N. Ereemeev, O.S. Dymshits, I.P. Alekseeva, A.A. Khubetsov, M.Ya. Tsenter, S.S. Zapalova, L.R. Basyrova, P.A. Loiko, A.A. Zhilin. *Opt. Spectrosc.*, **132**, 152–158 (2024). DOI: 10.61011/EOS.2024.02.58450.5815-23
- [18] P. Scherrer. *J. Abh. Akad. Wiss. Gött., Math.-Phys. Kl.*, **2**, 98 (1918).
- [19] I. Alekseeva, A. Baranov, O. Dymshits, V. Ermakov, V. Golubkov, M. Tsenter, A. Zhilin. *J. Non-Cryst. Solids*, **357**, 3928 (2011). DOI: 10.1016/j.jnoncrysol.2011.08.011
- [20] I.P. Alekseeva, O.S. Dymshits, V.A. Ermakov, A.A. Zhilin, M.Ya. Tsenter. *Glass Phys. Chem.*, **39**, 113–123 (2013). DOI: 10.1134/S1087659613020028
- [21] I. Alekseeva, O. Dymshits, V. Ermakov, V. Golubkov, A. Mal'yarevich, M. Tsenter, A. Zhilin, K. Yumashev. *Phys. Chem. Glas. Eur. J. Glass Sci. Technol. B*, **53**, 167–180 (2012).
- [22] V. Mohaček-Grošev, M. Vrankić, A. Maksimović, V. Mandić. *J. Alloys Compd.*, **697**, 90–95 (2017). DOI: 10.1016/j.jallcom.2016.12.116
- [23] I.P. Alekseeva, N.M. Belyaevskaya, Ya.S. Bobovich, M.Ya. Tsenter, T.I. Chuvaeva. *Opt. Spectrosc.*, **45**, 175 (1978).
- [24] V.F. Lebedev, V.M. Marchenko, N.N. Mel'nik, V.A. Myzina. *Quantum Electron.*, **26**, (7) 617–620 (1996). DOI: 10.1070/QE1996v026n07ABEH000738
- [25] B.M. Loeffler, R.G. Burns, J.A. Tossell, D.J. Vaughan, K.H. Johnson. *Proceedings of the Fifth Lunar Conf., Supplement 5*, *Geochim. Cosmochim. Acta*, **3**, 3007 (1974).
- [26] M. Kumar, A. Uniyal, A.P.S. Chauhan, S.P. Singh. *Bull. Mater. Sci.*, **26**, 335–341 (2003). DOI: 10.1007/BF02707456
- [27] L.E. Bausá, I. Vergara, J. García-Solé, W. Strek, P.J. Deren. *J. Appl. Phys.*, **68**, 736 (1990). DOI: 10.1063/1.346807
- [28] E.M. Dianov, V.F. Lebedev, Yu.S. Zavorotnyi. *Quantum Electron.*, **31**, (2) 187–188 (2001). DOI: 10.1070/QE2001v031n02ABEH001915
- [29] K. Morinaga, H. Yoshida, H. Takebe. *J. Am. Ceram. Soc.*, **77**, 3113 (1994). DOI: 10.1111/j.1151-2916.1994.tb04557.x
- [30] S.A. Basun, T. Danger, A.A. Kaplyanskii, D.S. McClure, K. Petermann, W.C. Wong. *Phys. Rev. B*, **54**, 6141 (1996). DOI: 10.1103/PhysRevB.54.6141
- [31] A. Sanchez, A.J. Strauss, R.L. Aggarwal, R.E. Fahey. *IEEE J. Quantum Electron.*, **24** (6), 1002 (1988). DOI: 10.1109/3.220
- [32] V.M. Khomenko, K. Langer, H. Rager, A. Fett. *Phys. Chem. Minerals*, **25**, 338–346 (1998). DOI: 10.1007/s002690050124
- [33] L.H.C. Andrade, S.M. Lima, A. Novatski, A.M. Neto, A.C. Bento, M.L. Baesso, F.C.G. Gandra, Y. Guyot, G. Boulon. *Phys. Rev. B*, **78**, 224202 (2008). DOI: 10.1103/PhysRevB.78.224202
- [34] M.J. Norman, L.D. Morpeth, J.C. McCallum. *Mater. Sci. Eng.*, **106** (3), 257–262 (2004). DOI: 10.1016/j.mseb.2003.09.032
- [35] A. Deepthy, M.N. Satyanarayan, K.S.R.K. Rao, H.L. Bhat. *J. Appl. Phys.*, **85** (12), 8332–8336 (1999). DOI: 10.1063/1.370679
- [36] P.F. Moulton, J.G. Cederberg, K.T. Stevens, G. Foundos, M. Koselja, J. Preclikova. *Opt. Mater. Express*, **9** (5), 2216 (2019). DOI: 10.1364/OME.9.002216
- [37] A. Sanchez, R.E. Fahey, A.J. Strauss, R.L. Aggarwal. *Opt. Lett.*, **11**, 363 (1986). DOI: 10.1364/ol.11.000363

Translated by D.Safin